Report

Cell Reports

Mono- and Digalactosyldiacylglycerol Lipids Function Nonredundantly to Regulate Systemic Acquired Resistance in Plants

Graphical Abstract

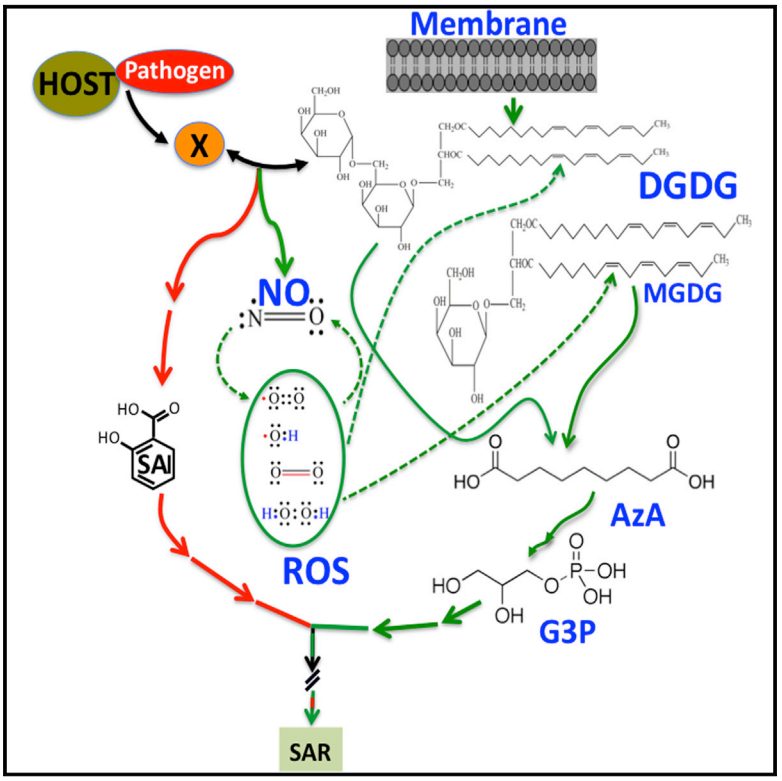

Highlights

Galactolipids (MGDG and DGDG) act nonredundantly in systemic acquired resistance (SAR)

DGDG is required for pathogen-responsive nitric oxide and salicylic acid accumulation

MGDG and DGDG contribute to the biosynthesis of the SAR signal azelaic acid

The α-galactose-β-galactose head group of DGDG is essential for SAR

Authors

Qing-ming Gao, Keshun Yu, ..., Aardra Kachroo, Pradeep Kachroo

Correspondence

apkach2@uky.edu (A.K.),
pk62@uky.edu (P.K.)

In Brief

The galactolipids monogalactosyldiacylglycerol (MGDG) and digalactosyldiacylglycerol (DGDG) constitute ~80% of total membrane lipids in plants. Gao et al. now show that these galactolipids function nonredundantly to regulate systemic acquired resistance (SAR). Furthermore, they show that the terminal galactose on the α-galactose-β-galactose head group of DGDG is critical for SAR.

Gao et al., 2014, Cell Reports 9, 1681–1691
December 11, 2014 ©2014 The Authors
http://dx.doi.org/10.1016/j.celrep.2014.10.069

Cell Reports
Report

Mono- and Digalactosyldiacylglycerol Lipids Function Nonredundantly to Regulate Systemic Acquired Resistance in Plants

Qing-ming Gao,[1] Keshun Yu,[1] Ye Xia,[1,4] M.B. Shine,[1] Caixia Wang,[1,2] DuRoy Navarre,[3] Aardra Kachroo,[1,*] and Pradeep Kachroo[1,*]
[1]Department of Plant Pathology, University of Kentucky, Lexington, KY 40546, USA
[2]Qingdao Agricultural University, Number 700, Changcheng Road, Chengyang District, Qingdao City 266109, PRC
[3]Agricultural Research Service, United States Department of Agriculture, Washington State University, Prosser, WA 99350, USA
[4]Present address: Department of Horticulture, University of Kentucky, Lexington, KY 40546, USA
*Correspondence: apkach2@uky.edu (A.K.), pk62@uky.edu (P.K.)
http://dx.doi.org/10.1016/j.celrep.2014.10.069

SUMMARY

The plant galactolipids monogalactosyldiacylglycerol (MGDG) and digalactosyldiacylglycerol (DGDG) have been linked to the anti-inflammatory and cancer benefits of a green leafy vegetable diet in humans due to their ability to regulate the levels of free radicals like nitric oxide (NO). Here, we show that DGDG contributes to plant NO as well as salicylic acid biosynthesis and is required for the induction of systemic acquired resistance (SAR). In contrast, MGDG regulates the biosynthesis of the SAR signals azelaic acid (AzA) and glycerol-3-phosphate (G3P) that function downstream of NO. Interestingly, DGDG is also required for AzA-induced SAR, but MGDG is not. Notably, transgenic expression of a bacterial glucosyltransferase is unable to restore SAR in *dgd1* plants even though it does rescue their morphological and fatty acid phenotypes. These results suggest that MGDG and DGDG are required at distinct steps and function exclusively in their individual roles during the induction of SAR.

INTRODUCTION

Systemic acquired resistance (SAR) is a form of defense response that protects plants against a broad spectrum of secondary infections by related or unrelated pathogens (reviewed in Shah and Zeier, 2013; Kachroo and Robin, 2013; Gao et al., 2014; Wendehenne et al., 2014). SAR involves the generation of a mobile signal in the primary leaves that, upon translocation to the distal tissues, activates defense responses resulting in broad-spectrum resistance. The production of the mobile signal occurs within 6 hr of primary pathogen infection, and the signal is then transferred to the distal uninfected tissues (Chanda et al., 2011). A quest for the SAR-inducing long-distance signal has led to the isolation of several factors that are required for SAR and/or confer SAR when applied exogenously (reviewed in Shah and Zeier, 2013; Kachroo and Robin, 2013; Gao et al., 2014; Wendehenne et al., 2014). Components of SAR include glycerol-3-phosphate (G3P; Chanda et al., 2011; Yu et al., 2013; Wang et al., 2014), the dicarboxylic acid azelaic acid (AzA; Jung et al., 2009), and the free radicals nitric oxide (NO) and reactive oxygen species (ROS) (Wang et al., 2014). Recent in vitro and in planta studies have shown that AzA is derived from the oxidation of C18 unsaturated fatty acids (FAs) that contain a double bond on C9 and that this process is facilitated by ROS (Zoeller et al., 2012; Yu et al., 2013; Wang et al., 2014). NO/ROS confer SAR in a concentration-dependent manner, and although ROS functions downstream of NO, it is required for pathogen-inducible NO accumulation (Wang et al., 2014). Different ROS species function additively to generate the FA-derived AzA, which in turn results in accumulation of the SAR inducer G3P (Wang et al., 2014; Wendehenne et al., 2014). Consequently, AzA is unable to confer SAR on mutants impaired in *GLY1*-encoded G3P dehydrogenase (G3Pdh) or *GLI1*-encoded glycerol kinase (GK) activities (Yu et al., 2013). Notably, the NO-ROS-AzA-G3P branch of SAR operates in parallel with salicylic acid (SA), a well-known regulator of SAR. Both branches are essential for the activation of SAR (Figure S1A). Consistent with this scheme of function, neither AzA nor G3P induces SA accumulation when applied alone or together with pathogen (Yu et al., 2013; Wang et al., 2014).

Galactolipids and cuticle have also been associated with SAR (Chaturvedi et al., 2008; Xia et al., 2010, 2012), although the underlying mechanism remains unknown. The plant galactolipids constitute ~80% of total membrane lipids, and of these, monogalactosyldiacylglycerol (MGDG) is considered to be the most abundant, accounting for ~50% of the total thylakoid lipids (Kelly and Dörmann, 2004). MGDG is synthesized by the monogalactosyl synthase 1 (MGD1)-mediated transfer of a galactose residue to diacylglycerol (Awai et al., 2001). A partial or complete defect in MGD1 reduces the MGDG level by ~42% (*mgd1-1*; Jarvis et al., 2000) or ~98% (*mgd1-2*; Kobayashi et al., 2007), respectively. Consistent with their MGDG level, *mgd1-1* plants show wild-type-like morphology, but the *mgd1-2* mutants germinate as albino (Kobayashi et al., 2007). MGDG is subsequently converted to digalactosyldiacylglycerol (DGDG) via digalactosyl

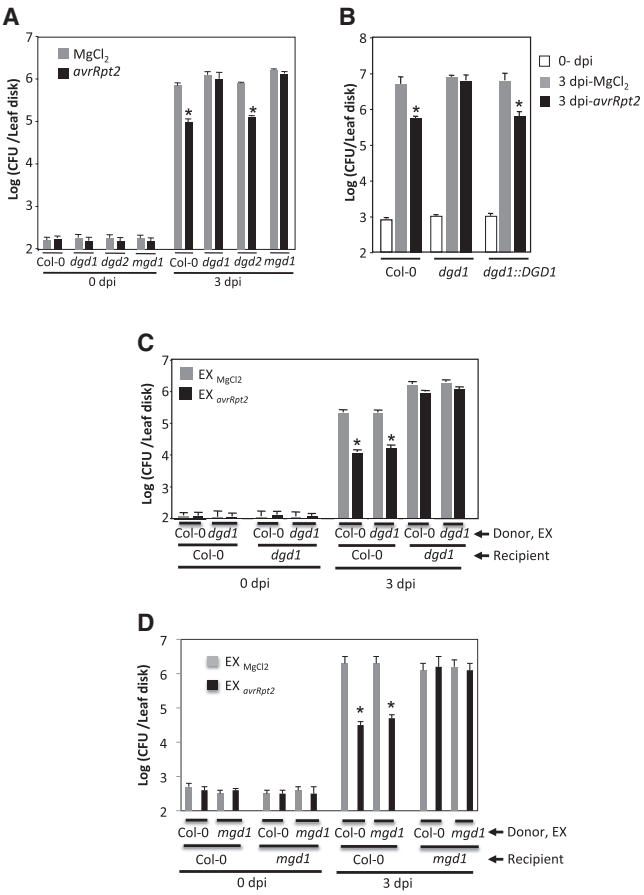

Figure 1. The *dgd1* Mutant Is Compromised in SAR

(A) SAR response in indicated genotypes. Primary leaves were inoculated with $MgCl_2$ (gray bars) or *Pst avrRpt2* (black bars), and the systemic leaves were inoculated 48 hr later with a virulent strain of *P. syringae*.

(B) SAR response in indicated genotypes. Transgenic *dgd1* plants constitutively expressing a wild-type copy of *DGD1* are designated *dgd1*::*DGD1*.

(C) SAR response in Col-0 and *dgd1* plants infiltrated with exudates collected from Col-0 or *dgd1* plants that were pretreated with either $MgCl_2$ (EX_{MgCl2}) or *Pst avrRpt2* ($EX_{avrRpt2}$).

(D) SAR response in Col-0 and *mgd1* plants infiltrated with EX_{MgCl2} or $EX_{avrRpt2}$ from Col-0 or *mgd1* plants.

All experiments were repeated at least two times with similar results. Error bars represent SD (n = 3 or 4). Asterisk denotes a significant difference (Student's t test).

synthase 1 (DGD1), which transfers another galactose residue to MGDG (Dörmann et al., 1999; Froehlich et al., 2001). Notably, wild-type-like levels of DGDG in *mgd1-1* plants suggest that either DGD1 can utilize other substrates in planta or the low MGDG levels in *mgd1-1* plants are sufficient for DGDG biosynthesis in these plants.

To determine the biochemical basis underlying involvement of galactolipids in SAR, we evaluated a role for MGDG and DGDG galactolipids in various steps leading to the induction of systemic immunity. We find that MGDG and DGDG regulate SAR at distinct steps and function nonredundantly. DGDG functions in SAR by contributing to pathogen-responsive NO biosynthesis. In contrast, MGDG regulates SAR via its effect on AzA, which functions downstream of NO. Our study highlights the importance of the axial hydroxyl group at C4 of DGDG galactose in NO biosynthesis and SAR. This study also highlights the similar function of lipids in the regulation of NO in plants and animals.

RESULTS

The *dgd1* Mutant Is Compromised in SAR

Consistent with an earlier report (Chaturvedi et al., 2008), we found that *mgd1* plants were compromised in SAR (Figure 1A). To examine the biochemical basis of this defect in the context of galactolipid pools, we analyzed SAR in *dgd* plants that accumulate reduced levels of DGDG. In *Arabidopsis*, two genes (*DGD1* and *DGD2*) are involved in the synthesis of DGDG, of which DGD1 is the major isoform impacting DGDG biosynthesis (Kelly et al., 2003; Figures S1B and S1C). Wild-type (WT) and *dgd1* plants were first inoculated with $MgCl_2$ or avirulent bacteria (*Pseudomonas syringae* pv. *tomato* [*Pst*] expressing *avrRpt2*) followed by a second inoculation with virulent bacteria on distal tissues at 48 hr after primary inoculation. Growth of the virulent bacteria was monitored at 0 and 3 days postinoculation (dpi) (Figure 1A). As expected, $MgCl_2$-infiltrated leaves of WT (Col-0 ecotype) plants supported more growth of the secondary virulent pathogen than the plants that were preinfected with *avrRpt2*, indicating appropriate induction of SAR (Figure 1A). In comparison, the *dgd1* mutant plants showed compromised SAR; plants infiltrated with $MgCl_2$ or *avrRpt2* bacteria were equally susceptible to the secondary virulent bacteria in the distal tissues. Unlike *dgd1*, the *dgd2* plants showed normal SAR, and this correlated with the detectable levels of DGDG in these plants (Figure S1B). Together, these data suggested that DGD1 is required for the proper induction of SAR and the compromised SAR in *dgd1* plants correlated with the reduced DGDG levels (Kelly et al., 2003; Figures S1B and S1C). Transgenic *dgd1* plants expressing a wild-type copy of *DGD1* (*dgd1::DGD1*) showed normal SAR (Figures 1B and S1D), suggesting that compromised SAR in *dgd1* plants was specifically associated with the *dgd1* mutation.

Next, we assessed whether DGDG was required for production or perception of the SAR mobile signal. We evaluated the response of WT and *dgd1* plants to vascular exudates collected from pathogen-inoculated WT and *dgd1* leaves. The WT or *dgd1* leaves were infiltrated with $MgCl_2$ or *avrRpt2* bacteria, and vascular exudates ($Ex_{MgCl2/avrRpt2}$) collected from the inoculated leaves were injected into the leaves of a fresh set of WT or *dgd1* plants. Distal leaves of plants infiltrated with $Ex_{MgCl2/avrRpt2}$ were then inoculated with virulent bacteria and proliferation of virulent bacteria monitored at 0 and 3 dpi (Figure 1C). As expected, $Ex_{avrRpt2}$ from WT plants conferred protection against virulent pathogen in WT plants, as did $Ex_{avrRpt2}$ from *dgd1* plants, suggesting that *dgd1* mutant plants were able to generate the SAR signals. In comparison, neither WT $Ex_{avrRpt2}$ nor *dgd1* $Ex_{avrRpt2}$ induced SAR in *dgd1* plants, suggesting that *dgd1* plants were unable to sense the SAR signals. We tested this further by assaying $Ex_{avrRpt2}$-induced SAR in *mgd1* plants, since they accumulate WT-like levels of DGDG (Figures S1B and S1C; Kelly et al., 2003). Interestingly, as in *dgd1*, *mgd1* $Ex_{avrRpt2}$ was able to confer SAR on WT plants, but not on *mgd1* plants (Figure 1D). Conversely, WT $Ex_{avrRpt2}$ was unable to confer SAR on *mgd1* plants. Together, these data

suggested that both *mgd1* and *dgd1* plants were able to make the SAR signal(s) but unable to respond to them.

The *dgd1* Mutant Is Impaired in the SA Branch of SAR

Recently, we showed that induction of SAR is dependent on two parallel pathways, one of which is regulated by SA (Figure S1A; Wang et al., 2014). To test the effect of *mgd1* and *dgd1* mutations on the SA pathway, we first evaluated the expression of the SA marker gene, *PR-1*, in mock- and *avrRpt2*-infected plants. Interestingly, compared to WT (Col-0) and *mgd1* plants, which showed comparable induction of *PR-1* expression, the *dgd1* plants showed significantly lower levels of *PR-1* in their inoculated leaves (Figure 2A). Similar results were obtained when we assayed *PR-1* levels in Col-0 and *dgd1* plants infiltrated with $Ex_{MgCl2/avrRpt2}$ from Col-0 plants (Figure S2A). These results suggested that *dgd1* plants were impaired in either pathogen-responsive SA accumulation or signaling. Therefore, we tested the basal and pathogen-responsive SA levels in *dgd1* plants. Although the *dgd1* plants accumulated WT-like levels of basal free SA and the SA glucoside (SAG), they contained significantly reduced free SA and SAG after pathogen infection (Figure 2B). In contrast and as expected, WT leaves infected with *avrRpt2* showed a significant increase in free SA and SAG (Figure 2B). Although the distal tissues of *dgd1* plants also showed a marked reduction in free SA level, they accumulated slightly higher levels of SAG compared to WT plants (Figure 2B), the biological significance of which remains unclear at this point. Congruent with their inability to accumulate SA after *avrRpt2* inoculation, the *dgd1* plants showed compromised local resistance to *avrRpt2 Pst* but displayed WT-like response to virulent bacteria (Figure 2C). Thus, the reduced pathogen-responsive *PR-1* expression of *dgd1* plants associated with their reduced SA levels and local R-mediated resistance.

To determine if the reduced accumulation of SA in *dgd1* plants was responsible for their defective SAR, we assayed SAR after SA treatment. Localized application of SA induced SAR in WT, but not *dgd1*, plants (Figure 2D). Next, we tested whether addition of SA to $Ex_{avrRpt2}$ improved the SAR response of *dgd1* plants. $Ex_{MgCl2/avrRpt2}$ collected from WT or *dgd1* plants was mixed with water or SA and injected into the leaves of a fresh set of WT and *dgd1* plants. Col-0 Ex_{MgCl2} + SA induced SAR on Col-0 plants, but not on *dgd1* plants (Figure S2B). In comparison, *dgd1* Ex_{MgCl2} + SA was unable to confer SAR on either Col-0 or *dgd1* plants. As seen above (Figure 1C), *dgd1* $Ex_{avrRpt2}$ conferred SAR on Col-0 plants, but not on *dgd1* plants. Both Col-0 and *dgd1* $Ex_{avrRpt2}$ + SA induced better SAR on Col-0 plants than $Ex_{avrRpt2}$ alone ($p < 0.05$), but not on *dgd1*. This suggested that although addition of SA to WT/*dgd1* $Ex_{avrRpt2}$ improved SAR in Col-0 plants, SA was unable to restore the SAR response to $Ex_{avrRpt2}$ in *dgd1* plants. To determine if this was due to reduced sensitivity to SA, we compared the expression of the SA-inducible marker *PR-1* in *dgd1* and WT plants. Similar levels of *PR-1* transcript were induced in response to SA in both Col-0 and *dgd1* plants (Figure S2C), suggesting that *dgd1* plants are as responsive to SA as WT plants. Together, these results suggested that although DGDG is required for pathogen triggered SA accumulation, the SAR defect in *dgd1* could not be entirely attributed to their inability to accumulate SA.

The *dgd1* Mutant Accumulates Normal JA Levels

Since *dgd1* plants are also impaired in photosynthesis (Klaus et al., 2002), it was possible that the defective SA accumulation was the consequence of a generalized defect in chloroplast (site of SA synthesis) biogenesis. We assessed this by monitoring pathogen-inducible JA accumulation in the *dgd1* plants, since JA synthesis also begins in the chloroplasts. The *dgd1* mutant plants accumulated JA in response to pathogen infection at levels comparable to those of WT plants (Figure 2E). We next compared total and free FA levels in WT and *dgd1* plants, because FAs not only are synthesized de novo in the chloroplast but also serve as a precursor for JA synthesis. The *dgd1* plants accumulated reduced levels of 16:3 FA (Figure S2D), which is consistent with their reduced DGDG pool (Figures S1B and S1C). In comparison, both *dgd2* and *dgd::DGD1* showed WT-like 16:3 levels. Normal JA levels in *dgd1* plants were consistent with their total as well as free 18:3 FA levels; like wild-type plants, the *dgd1* plants showed increased accumulation of free 18:3 in response to pathogen infection (Figure 2F). Together, these results suggested that the defect in pathogen-induced SA accumulation of *dgd1* plants was unlikely to be associated with a generalized defect in chloroplast function.

Since *dgd1* showed impaired import of nuclear proteins into plastids (Chen and Li, 1998), it was possible that the reduced SA accumulation in these plants was associated with altered import of proteins involved in SA biosynthesis. We first assayed the transcript levels of nuclear-encoded genes that were induced in response to pathogen infection and contributed to SA or JA levels. Notably, unlike WT and *mgd1* plants, *dgd1* mutant plants showed significantly reduced induction of *EDS5* and *SID2*, which are involved in transport or biosynthesis of SA, respectively (Figure 2G). Likewise, *Pst avrRpt2*-inoculated *dgd1* plants showed no induction of *EDS1* and *PAD4* genes, which indirectly contribute to SA biosynthesis (Figure 2H). In comparison, the induced levels of JA pathway genes *LOX3* and *OPR3* in *dgd1* plants were comparable to the WT plants (Figure 2G). Unlike *dgd1*, the *mgd1* plants showed WT-like induction of *EDS5* and *SID2* genes and higher-than-WT induction of *LOX3* and *OPR3* (Figure 2G). Together, these results suggest that reduced SA levels in *dgd1* plants are likely due to their inability to induce the transcription of genes involved in SA biosynthesis.

The *dgd1* and *mgd1* Plants Are Compromised in Pathogen-Induced G3P and AzA Levels

We next assayed if the SAR defect in *dgd1* was associated with deficiencies in other chemical signals of the NO-derived branch of SAR (see Figure S1A). We first assayed G3P levels, since it acts downstream of NO, ROS, and AzA (Figure S1A; Chanda et al., 2011; Yu et al., 2013, Wang et al., 2014). As shown earlier (Chanda et al., 2011; Yu et al., 2013; Wang et al., 2014), *avrRpt2*-infected WT plants accumulated ~3- to 4-fold higher levels of G3P in their vascular exudates (Figure 3A). In comparison, pathogen-infected *dgd1* plants did not accumulate higher- than-basal levels of G3P. This was also the case for *mgd1* plants (Figure 3A). Together, these results suggested that the compromised SAR in *mgd1* and *dgd1* plants might be associated with

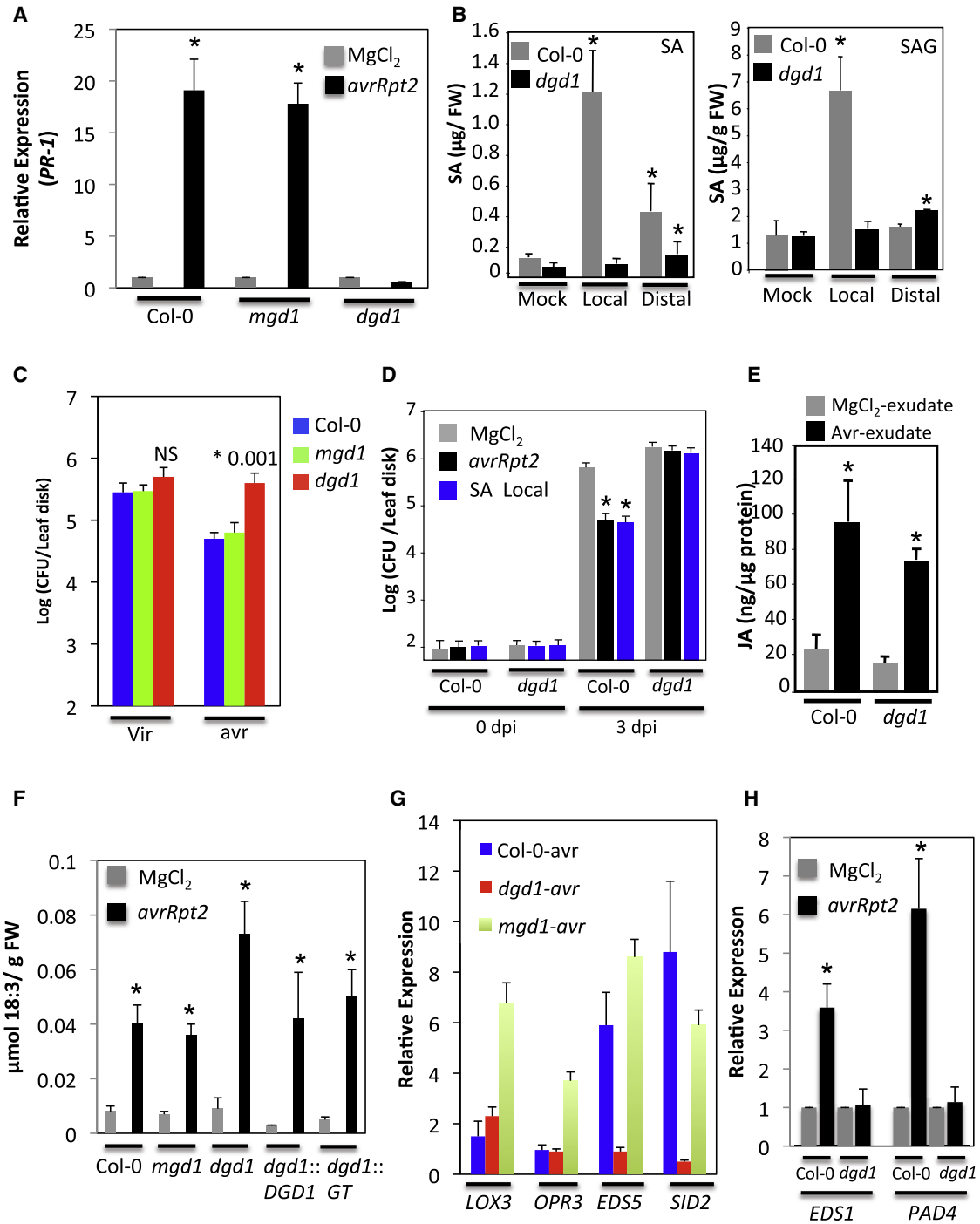

Figure 2. The *dgd1* Mutant Is Impaired in Pathogen-Induced SA Accumulation, but Not JA

(A) Quantitative RT-PCR analysis showing relative expression levels of *PR-1* in mock ($MgCl_2$)- and *avrRpt2*-inoculated local leaves from Col-0 (WT), *mgd1*, and *dgd1* plants.

(B) SA and SAG levels in Col-0 and *dgd1* plants inoculated with $MgCl_2$ or *P. syringae* expressing *avrRpt2*. FW indicates fresh weight.

(C) Local resistance response of Col-0 (WT), *mgd1* and *dgd1* plants to virulent (DC3000) and avirulent (*avrRpt2*) *Pst* bacteria (10^4 colony-forming units ml^{-1}). NS indicates not significant.

(D) SAR response in Col-0 and *dgd1* plants locally infiltrated with $MgCl_2$, *Pst avrRpt2*, or SA (500 µM). The virulent *Pst* DC3000 was inoculated 24 hr after local treatments.

(E) JA levels in petiole exudates collected from Col-0 and *dgd1* plants infiltrated with $MgCl_2$ (EX_{MgCl2}) or *Pst* expressing *avrRpt2* ($EX_{avrRpt2}$).

(F) Free 18:3 levels in indicated genotypes 24 hr postinfiltration of $MgCl_2$ or *avrRpt2*.

(legend continued on next page)

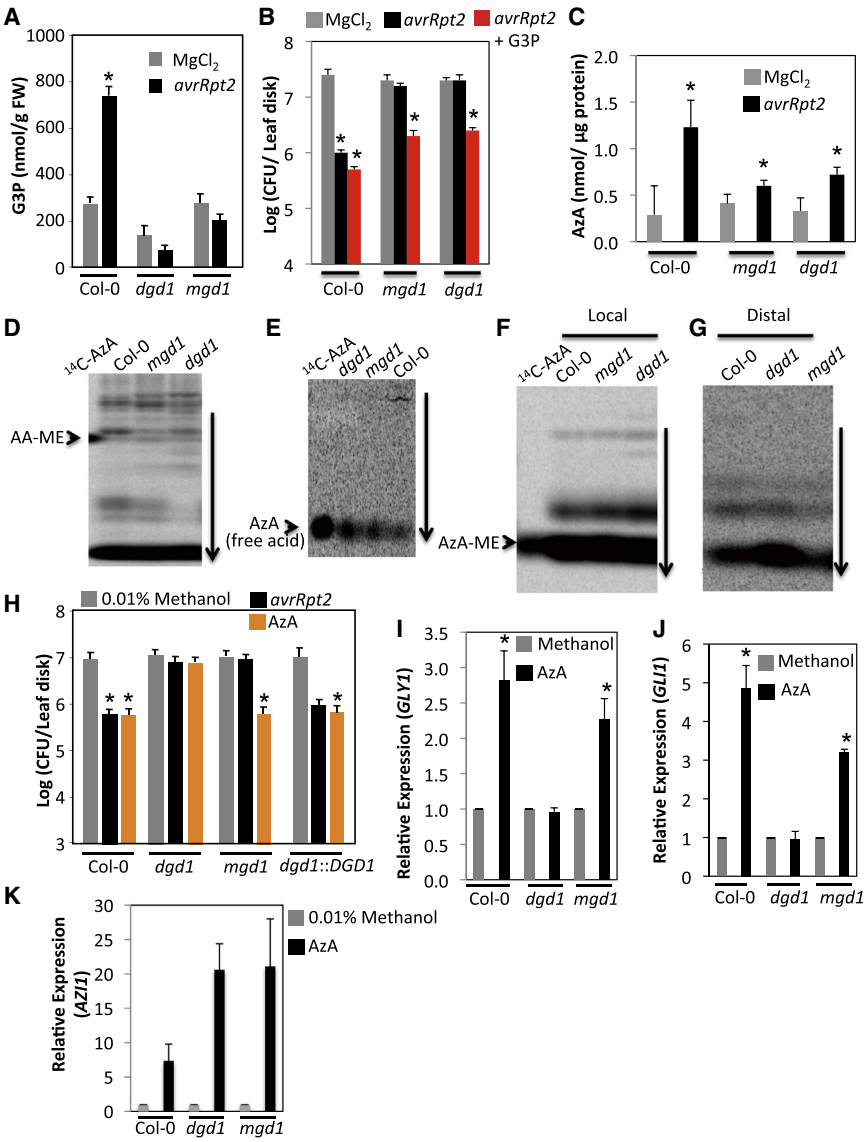

Figure 3. Exogenous G3P Complements Defective SAR in *mgd1* and *dgd1* Plants

(A) G3P levels in wild-type (Col-0), *mgd1*, and *dgd1* leaves at 24 hr after mock ($MgCl_2$) or pathogen (*avrRpt2*) infections.

(B) SAR response in Col-0, *mgd1*, or *dgd1* plants treated locally with $MgCl_2$, *avrRpt2*, or *avrRpt2* + 100 µm G3P.

(C) AzA levels in petiole exudates collected from Col-0, *mgd1*, or *dgd1* plants at 24 hr post-infiltration with $MgCl_2$ or *Pst avrRpt2*.

(D and E) Autoradiographs of TLC plates, samples analyzed on silica TLC using hexane/MTBE/acetic acid (80:20:1, by vol for D; 65:35:1, by vol for E solvent systems). Vertical arrows indicate direction of the runs. (D) Methyl esters of extracts from leaves infiltrated with ^{14}C-18:1 were analyzed together with ^{14}C-AzA methyl ester (AzA-ME) as standard. ^{14}C-containing products in leaves at 24 hr posttreatment are shown. (E) Comigration of ^{14}C-18:1-derived AzA with ^{14}C-AzA standard. Products corresponding to ^{14}C-AzA in (D) were extracted, hydrolyzed, and analyzed together with ^{14}C-AzA standard.

(F and G) Autoradiographs of TLC plates showing ^{14}C-AzA-derived products. Samples were analyzed on silica TLC plates using hexane/MTBE/acetic acid solvent systems (80:20:1, by volume). Vertical arrows indicate direction of the runs. Arrowheads indicate positions of the ^{14}C-AA methyl ester (ME). (F) TLC plate analysis of extracts prepared from ^{14}C-AzA-infiltrated (local) leaves sampled at 24 hr posttreatment. (G) TLC plate analysis of extract prepared from distal leaves of ^{14}C-AzA-infiltrated plants shown in (F). Samples containing equal disintegrations per minute (quantified using scintillation counts) from local and distal leaves were loaded.

(H) SAR response in Col-0, *mgd1*, or *dgd1* plants treated locally with 0.01% methanol or AzA for 24 hr prior to inoculation of distal leaves with a virulent strain of *P. syringae*.

(I–K) Real-time quantitative RT-PCR analysis showing fold increase in expression levels of *GLY1* (I), *GLI1* (J), or *AZI1* (K) in AzA-treated (1 mM) Col-0, *mgd1*, or *dgd1* plants in relation to plants treated with 0.01% methanol. Leaves were sampled 24 hr posttreatments.

All experiments were repeated at least two times with similar results. Error bars in (A)–(C) and (H)–(K) represent SD (n = 4). Asterisk denotes a significant difference (Student's t test).

their inability to accumulate G3P in response to pathogen infection. We tested this further by assaying SAR in G3P-treated *mgd1* and *dgd1* plants. Interestingly, exogenous G3P restored SAR in both *mgd1* and *dgd1* plants, suggesting that their compromised SAR was indeed associated with the inability to accumulate G3P and that these plants were defective in a step upstream of G3P (Figure 3B).

Previously, we showed that AzA acts upstream of G3P and confers SAR by increasing G3P levels (Yu et al., 2013). Therefore, we analyzed pathogen-responsive AzA levels in *mgd1* and *dgd1* plants. The *avrRpt2*-infected *mgd1* and *dgd1* plants accumulated significantly lower levels of AzA as compared to WT plants (Figure 3C). Given that AzA is derived from C18 unsaturated FAs containing a double bond at C9 (Zoeller et al., 2012; Yu et al.,

(G) Quantitative RT-PCR analysis showing relative induction of indicated genes in *avrRpt2* infected Col-0, *mgd1*, and *dgd1* plants compared to $MgCl_2$ (mock)-inoculated respective genotypes. Leaves were sampled 24 hr postinoculation.

(H) Quantitative RT-PCR analysis showing relative induction of *EDS1* and *PAD4* genes in *avrRpt2* infected Col-0 and *dgd1* plants compared to $MgCl_2$ (mock)-inoculated respective genotypes. Leaves were sampled 24 hr postinoculation.

All experiments were repeated at least two times with similar results. Error bars represent SD (n = 3 or 4). Asterisk denotes a significant difference (Student's t test).

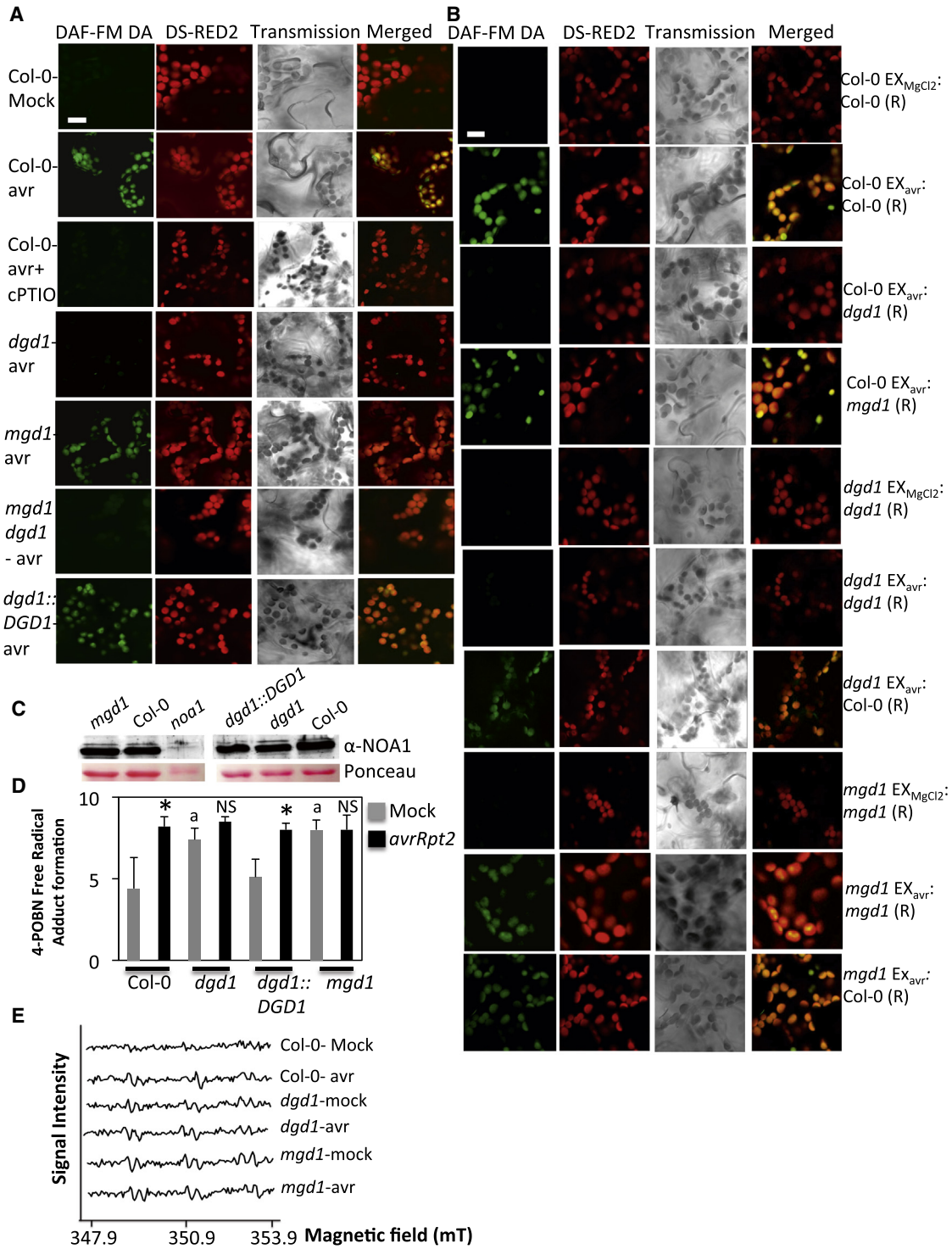

Figure 4. The *dgd1* Mutant Is Impaired in Pathogen-Induced NO Accumulation

(A) Confocal micrographs showing pathogen-induced NO accumulation in indicated genotypes at 12 hr postinoculation. The leaves were infiltrated with $MgCl_2$ (mock) or *avrRpt2 Pst,* with or without c-PTIO (500 μM). Scale bar, 10 μm.

(B) Confocal micrographs showing NO accumulation in indicated genotypes postinoculation with petiole exudates collected from $MgCl_2$ (EX_{MgCl2})- or *avrRpt2* (EX_{avr})-infected Col-0, *mgd1,* or *dgd1* plants. Scale bar, 10 μm. "R" indicates genotype that received the EX.

(C) Protein immunoblot showing NOA1 levels in total protein extracts from indicated genotypes. Ponceau-S staining of the immunoblot was used as the loading control. Equal amount of total proteins were also loaded for *noa1*, which accumulates reduced levels of RUBISCO (Mandal et al., 2012).

(legend continued on next page)

2013), and because *mgd1* and *dgd1* plants accumulate normal levels of free 18:3 FA (Figure 2F), it was possible that these mutants are unable to hydrolyze the C9 double bond that is required for the conversion of FA to AzA. To test this, we monitored the in planta conversion of ^{14}C-18:1 to AzA in *mgd1* and *dgd1* plants. We infiltrated ^{14}C-labeled 18:1 (^{14}C at C-1 position) into leaves of WT, *mgd1*, and *dgd1* plants and analyzed the methylated leaf extracts by thin layer chromatography (TLC). The TLC analysis showed a band corresponding to ^{14}C-AzA dimethyl ester (ME) (Figure 3D). This band was extracted from the TLC plates, demethylated to obtain the free acid form, and rerun on a new TLC plate (Figure 3E). The band corresponding to AzA control in the first TLC run comigrated with the AzA standard in the second TLC run (Figure 3E), thus arguing that *mgd1* and *dgd1* plants were not affected in conversion of C18 unsaturated FAs to AzA.

This did not, however, rule out a possible defect in the uptake and/or transport of AzA in *mgd1* and *dgd1* plants. To test this, we infiltrated WT, *mgd1*, and *dgd1* leaves with ^{14}C-AzA, prepared methylated leaf extracts at 24 hr postinfiltration, and analyzed them on TLC. As shown earlier (Yu et al., 2013), a large portion of the radiolabel was present as AzA in addition to several other minor derivatives in WT plants (Figure 3F). The pattern and relative levels of AzA and its derivatives in *mgd1* and *dgd1* plants were similar to WT plants (Figures 3F and S2E), suggesting that mutations in *MGD1* or *DGD1* did not alter the uptake or derivatization of AzA in the infiltrated leaves. Likewise, analysis of distal tissues of *mgd1* and *dgd1* mutants showed WT-like profile of AzA derivatives (Figure 3G) and WT-like levels of total ^{14}C-AzA (Figure S2E). Together, these results suggest that *mgd1* and *dgd1* plants are not altered in the uptake or transport of AzA or conversion of C18 FA to AzA. Thus, reduced levels of AzA in *mgd1* and *dgd1* plants were likely associated with their reduced MGDG and DGDG levels, respectively. Notably, this was not associated with a reduced free FA pool; both *mgd1* and *dgd1* plants accumulated WT-like levels of free 18:3 after pathogen infection (Figure 2F).

Based on the above results, we expected that exogenous treatment with AzA would compensate for the reduced AzA and confer SAR in *mgd1* and *dgd1* plants. AzA was applied locally, and the response to virulent bacteria was monitored in distal tissues. As expected, AzA-induced SAR in the systemic tissues of WT plants (Figure 3H). Intriguingly, although AzA also induced SAR in *mgd1* plants, it was unable to do so in *dgd1* plants (Figure 3H). This, together with the fact that both *mgd1* and *dgd1* plants accumulated reduced levels of G3P and that G3P was able to confer SAR in both these mutants, suggested that *DGD1*-derived DGDG galactolipids were likely involved in AzA-induced accumulation of G3P. To address this, we first assayed AzA-mediated SAR in *dgd1::DGD1* plants and found these to respond normally to AzA; the *dgd1*::*DGD1* plants showed WT-like SAR to exogenous AzA (Figure 3H). Next, we evaluated AzA-mediated transcriptional upregulation of the G3P biosynthesis genes *GLY1* and *GLI1*, which is associated with an AzA-mediated increase in G3P levels (Yu et al., 2013). Exogenous AzA application induced *GLY1* and *GLI1* expression in WT and *mgd1* plants, though *GLI1* transcript levels in *mgd1* were consistently lower compared to those in WT plants (Figures 3I and 3J). Notably, exogenous AzA was unable to induce expression of *GLY1* or *GLI1* genes in *dgd1* plants (Figures 3I and 3J), which correlated with the inability of AzA to confer SAR in *dgd1* plants. To determine if *dgd1* plants were able to respond to AzA, we analyzed the expression of AzA-responsive gene *AZI1* in these plants (Jung et al., 2009). AzA-treated *dgd1* plants showed high expression of *AZI1* (Figure 3K), suggesting that *dgd1* plants were able to sense AzA but unable to induce SAR in response to AzA. Together, these results suggest that the inability of AzA to induce *GLY1/GLI1* expression and confer SAR on *dgd1* mutant was likely associated with the reduced pool of DGDG galactolipids in *dgd1* plants.

DGDG Is Required for NO Biosynthesis and Accumulation

We recently showed that NO and ROS act upstream of AzA to confer SAR (Wang et al., 2014). This and reduced accumulation of AzA in *dgd1* and *mgd1* mutants prompted us to analyze NO and ROS levels in these plants. Analysis of NO levels was carried out using the NO-sensitive dye 4-amino-5-methylamino-2,7-difluorofluorescein diacetate (DAF-FM DA). Confocal microscopy of *Pst avrRpt2*-infected leaves detected increased DAF-FM DA staining 24 hr postinoculation (detected as green fluorescence) of Col-0 leaves compared to mock-inoculated or NO scavenger carboxy-PTIO (2-(4-carboxyphenyl)-4,4,5,5-tetramethylimidazoline-1-oxyl-3-oxide)-treated plants (Figure 4A). Unlike in WT plants, NO could not be detected in pathogen-infected *dgd1* plants (Figure 4A). However, NO accumulation was restored in the *dgd1::DGD1* complemented lines (Figure 4A), which were also SAR competent (Figures 1B and 3H). Interestingly, unlike *dgd1*, the pathogen infected *mgd1* plants did accumulate NO (Figure 4A). To test whether NO accumulation was primarily associated with DGDG lipids, we evaluated NO levels in *mgd1 dgd1* double-mutant plants. The double mutant, which shows *dgd1*-like morphology (Figure S3A), did not show detectable NO accumulation after pathogen infection like the *dgd1* single mutant (Figure 4A). This suggested that *dgd1* was epistatic to *mgd1* and that DGDG was perhaps required for normal biosynthesis and/or accumulation of NO. To determine if the defect was associated with biosynthesis or accumulation, we assayed NO accumulation in *dgd1* plants treated with the NO donors sodium nitroprusside (SNP) or 2-(N,N-diethylamino)-diazenolate-2-oxide (DETA-NONOate) or the nitrous oxide donor SULFO-NONOate (negative control) (Figure S3B). Notably, *dgd1* plants showed WT-like NO staining after SNP or DETA-NONOate treatments, suggesting that *dgd1* plants were likely affected in biosynthesis of NO, but not its accumulation.

(D) Electron spin resonance (ESR) spectrometry assay showing relative levels of 4-POBN adduct in local tissues of mock and *avrRpt2* inoculated Col-0, *mgd1*, *dgd1*, and *dgd1::DGD1* plants. The leaves were sampled at 12 hr postinoculation.

(E) ESR spectrometry spectra of carbon centered radical levels in mock- and *avrRpt2*-inoculated leaves of Col-0, *mgd1*, and *dgd1* plants.

For (A) and (B), at least six independent leaves were stained with DAF-FM DA and analyzed in three independent experiments with similar results. Experiments shown in (C)–(E) were repeated at least two times with similar results. Error bars in (D) represent SD (n = 3). Asterisk denotes a significant difference (Student's t test).

Intriguingly, even though *dgd1* plants were impaired in the biosynthesis of multiple SAR signals like NO, AzA, and G3P, the $Ex_{avrRpt2}$ from *dgd1* plants were fully capable of inducing SAR on WT plants (Figure 1C). One possibility was that *dgd1* $Ex_{avrRpt2}$ contained signals that act upstream of NO and can induce NO biosynthesis in WT plants. To test this, we evaluated NO levels in WT and *dgd1* plants treated with $Ex_{MgCl2/avrRpt2}$ from WT and *dgd1* plants. As an additional control, we also included *mgd1* plants in this analysis. As predicted, WT $Ex_{avrRpt2}$ was able to induce NO biosynthesis in WT and *mgd1* plants, but not *dgd1* plants (Figure 4B). Likewise, *mgd1* $Ex_{avrRpt2}$ induced NO accumulation in *mgd1* and WT plants. Notably, *dgd1* $Ex_{avrRpt2}$ induced NO biosynthesis in WT, but not *dgd1*, plants. Together, these results suggested that DGD1, and thereby DGDG lipids, are essential for NO synthesis, but not for generating the SAR signal(s). These results further suggest that such a signal(s) from *dgd1* is able to activate NO synthesis, and thereby SAR, in a plant that contains normal DGDG levels. One plausible reason for impaired NO accumulation in *dgd1* plants could be that it is affected in the plastidal import and/or stability of NOA1, which is an indirect major contributor of pathogen-responsive NO accumulation. However, comparison of NOA1 levels in WT, *mgd1*, *dgd1*, and *dgd1:DGD1* plants did not detect significant differences in NOA1 levels in these plants (Figure 4C).

Since ROS act downstream of NO, we monitored ROS levels in the infected tissues of *dgd1* and *mgd1* mutants using electron spin resonance spectrometry (ESRS). ESRS using α-(4-pyridyl *N*-oxide)-*N*-*tert*-butylnitrone (POBN), which detects hydroxyl and carbon-centered radicals, detected increased accumulation of free radicals in the *Pst avrRpt2*-infected tissues of WT plants (Figures 4D and 4E). Quantification of POBN trapped free radicals in local tissues of *dgd1* and *mgd1* plants showed significantly higher basal levels, which did not increase further after *Pst avrRpt2* inoculation (Figures 4D and 4E). In comparison, *dgd1::DGD1* plants showed WT-like basal and pathogen-induced POBN trapped free radicals (Figure 4D). Higher basal ROS levels in *dgd1* plants were unexpected, since they are unable to accumulate NO that acts upstream of ROS (Wang et al., 2014). To test if higher basal ROS in *mgd1* and *dgd1* plants were due to their impaired photosynthesis, we assayed their sensitivity to paraquat (methyl viologen), an agent that promotes the formation of ROS by inhibiting electron transport during photosynthesis. The plants were treated by placing a 10 μl droplet of 10 to 20 μM paraquat on individual leaves, and the lesion size was monitored 48 hr posttreatment. The *dgd1* and *mgd1* plants developed larger lesions, suggesting that they are defective in the regulation/sequestration of ROS derived from photosynthetic electron transport (Figures S3C and S3D). Consistent with this result, both *mgd1* and *dgd1* plants showed increased expression of antioxidant genes (Figure S3E). This result further suggests that increased expression of antioxidants genes in *mgd1* and *dgd1* plants could be responsible for scavenging the excess ROS induced upon pathogen infection. In contrast to paraquat, *dgd1* and *mgd1* plants showed WT-like sensitivity to exogenous H_2O_2 (Figures S3F). Thus, the impaired photosynthesis in *mgd1* and *dgd1* plants was likely responsible for their higher basal ROS levels.

Transgenic Expression of Bacterial Glucosyltransferase Rescues Morphological and FA Phenotype, but Not SAR Phenotype, of *dgd1* Plants

To determine the importance of the galactose sugar moiety in DGDG for SAR, we evaluated the response of transgenic *dgd1* plants expressing a glycosyltransferase (*GT*) gene from the photosynthetic bacteria *Chloroflexus aurantiacus*. The transgenic expression of *GT* introduces glucose instead of galactose on the MGDG, resulting in formation of β-glucose-β-galactose diacylglycerol (Hölzl et al., 2006; Figures 5A and S1B). Notably, WT-like morphology could be restored in transgenic *dgd1* plants expressing either the bacterial *GT* (*dgd1::GT*) or native *DGD1* (*dgd1::DGD1*) (Figure 5B; Hölzl et al., 2006). Furthermore, transgenic expression of either *GT* or *DGD1* was able to normalize 16:3 levels in *dgd1* plants (Figure S2D). Interestingly, unlike native *DGD1*, the bacterial *GT* was unable to restore SAR in *dgd1* plants (Figure 5C). Pathogen-infected *dgd1::GT* plants accumulated nominal NO at levels significantly lower than those in pathogen-infected WT or *dgd1:DGD1* plants (Figure 5D). Similarly, compared to WT or *dgd1:DGD1* plants, pathogen-induced *PR-1* expression was only slightly higher in *dgd1::GT* plants (Figure S3G). The small increase of NO in *dgd1::GT* plants was insufficient to increase their AzA levels; *dgd1::DGD1* plants accumulated WT-like levels of AzA in response to pathogen infection, whereas both *dgd1* and *dgd1::GT* plants contained much lower AzA levels (Figure 5E). Furthermore, reduced accumulation of AzA did not associate with free FA pool, since *dgd1::GT* plants accumulated WT-like levels of free 18:3 (Figure 2F). Thus, even though *dgd1::GT* plants did exhibit a nominal increase in NO levels and *PR-1* expression in response to pathogen infection, this slight increase was clearly insufficient to confer SAR. To reconfirm this, we assayed SA-mediated SAR in *dgd::GT* plants, since exogenous SA would require functional NO-ROS-AzA-G3P branch to confer SAR (Wang et al., 2014). As predicted, exogenous SA was unable to confer SAR on *dgd1::GT* plants (Figure 5F). Together, these results suggest that the α-galactose-β-galactose head group is essential for normal induction of the NO-ROS-AzA-G3P branch of the SAR pathway as well as AzA-conferred SAR.

DISCUSSION

Galactolipids are one of the most abundant classes of lipids in plants, constituting ~80% of total membrane lipids in *Arabidopsis*. Although *Arabidopsis* leaves contain a higher proportion of MGDG compared to DGDG, the total and relative levels of these two galactolipids can vary in other plants (Christensen, 2009). Notably, in addition to serving as important constituents of chloroplastic membranes, galactolipids have also been shown to have other unique functions and are often associated with the medicinal and nutritional properties of vegetable plants (Christensen, 2009). For example, MGDG containing 18:3/18:3 or 16:3/18:3 FAs isolated from spinach leaves has antitumor activity (Wang et al., 2002). In this regard, it is interesting to note that MGDG and DGDG play a very specific role in plant defense leading to the induction of SAR (Figure S4). This is based on the specific phenotypes of *mgd1* and *dgd1* plants; *mgd1*

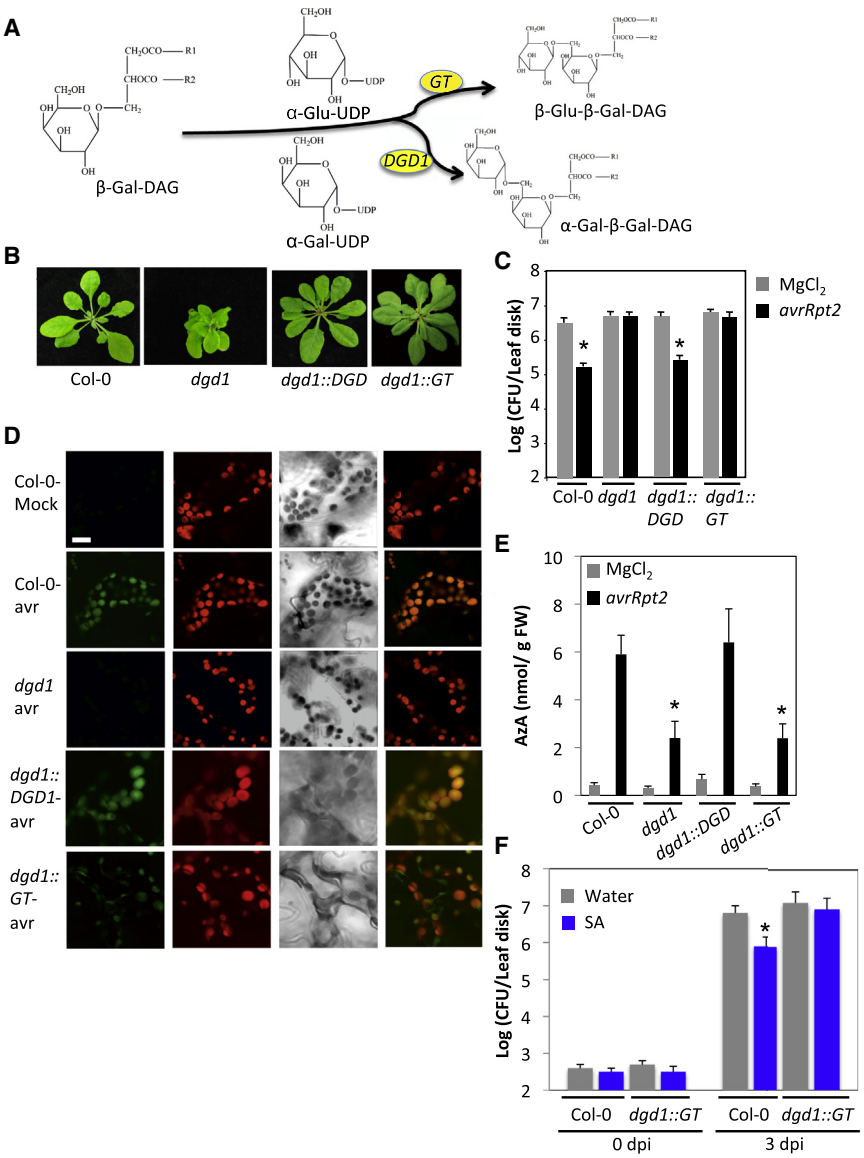

Figure 5. Transgenic Expression of Bacterial Glucosyltransferase Restores Morphology in *dgd1* Plants but Not SAR Phenotype

(A) Chemical structures and enzymatic steps catalyzed by the bacterial glucosyltransferase (GT) and DGD1 enzymes. Glu and gal indicate glucose and galactose sugars, respectively.

(B) Typical morphological phenotype of 4-week-old plants.

(C) SAR response in indicated genotypes treated locally with $MgCl_2$ (gray bars) or *avrRpt2 Pst* (black bars).

(D) Confocal micrographs showing pathogen-induced NO accumulation in indicated genotypes at 12 hr postinoculation. The leaves were infiltrated with $MgCl_2$ (mock) or *avrRpt2 Pst*, and at least six independent leaves were stained with DAF-FM DA and analyzed in three independent experiments with similar results. Scale bar, 10 μm.

(E) AzA levels in mock- ($MgCl_2$) or *avrRpt2 P. syringae* (Avr)-inoculated leaves of Col-0, *mgd1*, or *dgd1* plants at 24 hr postinoculation.

(F) SAR response in Col-0 or *dgd1* plants treated locally with water or 500 μM SA for 24 hr prior to inoculation of distal leaves with virulent *Pst*.

All experiments were repeated at least two times with similar results. Error bars in (C), (E), and (F) represent SD (n = 3 or 4). Asterisk denotes a significant difference (Student's t test).

plants, which accumulate WT-like levels of DGDG, are impaired in pathogen-induced ROS and AzA accumulation, but not NO levels or induction of the SA signaling marker, *PR-1*. In comparison, *dgd1* plants, which are drastically reduced in DGDG and contain WT levels of MGDG, are unable to accumulate NO or SA after pathogen infection. Thus, DGDG is required at an early step during SAR signaling and appears to link the NO- and SA-derived branches of this pathway.

The inability of *dgd1* plants to accumulate SA after pathogen infection is associated with reduced induction of the nuclear genes *SID2* and *EDS5*, which regulate SA biosynthesis or its export from the chloroplast, respectively. Notably, DGDG is also required for AzA-mediated induction of *GLY1* and *GLI1* genes. Consequently, exogenous AzA, which induced high expression of *GLY1* and *GLI1* genes and conferred SAR in *mgd1* plants, was unable to do so in *dgd1* plants. Thus, DGDG, which is synthesized in the outer envelope of plastids (Froehlich et al., 2001), might be important for retrograde signaling between the chloroplast and nucleus, since it regulates the expression of nuclear genes. Conversely, it is possible that impaired SA biosynthesis in chloroplast might result in the feedback suppression of nuclear genes directly or indirectly responsible for maintaining the pathogen-induced SA pool. Regardless, these results show that pathogen-activated signaling resulting in induction of the SA pathway is regulated by chloroplastic DGDG levels (Figure S5A).

The critical role of DGDG in pathogen-induced NO and SA production, and thereby SAR, is further reiterated by the SAR-defective phenotype of the *dgd1::GT*, which express a bacterial glucosyltransferase that adds a glucose sugar on MGDG. These plants contain a WT-like proportion of dihexosyldiacylglycerol, which is sufficient to rescue the morphological and FA defects of the *dgd1* mutant, but not SAR. Notably, unlike SAR, the *dgd1::GT* plants are partially restored in their photosynthetic efficiency (Hölzl et al., 2006), suggesting that induction of SAR has an absolute requirement for DGDG, and replacement of terminal galactose with glucose is unable to complement this defect. The significance of this result is further evident by the fact that galactose and glucose sugars are stereoisomers and only differ in the presence of an axial hydroxyl group at C4 of galactose. It is

possible that interaction involving this axial hydroxyl group of galactose confers a structural feature that allows DGDG to associate with membrane proteins, cofactors, or other FA/lipid molecules.

Interestingly, even though *mgd1* and *dgd1* plants were impaired in the biosynthesis of multiple SAR signals, the petiole exudates obtained from these plants were fully capable of inducing SAR on WT plants. This was especially true for *dgd1* plants, which are impaired in the biosynthesis of all major signals associated with SAR. These results suggest that *mgd1* and *dgd1* are able to make the SAR signal(s) but unable to respond to them. Thus, MGDG and DGDG lipids could play a role in the perception of the SAR signals. An alternate possibility is that *mgd1* and *dgd1* plants are able to make SAR signal(s) that act upstream of the SA-NO branch point, which in turn are sufficient to initiate SAR in the presence of WT-like levels of MGDG and DGDG (Figure S4).

Clearly, both MGDG and DGDG are required to generate sufficient AzA and in turn induce SAR, since *mgd1* (containing WT levels of DGDG) as well as *dgd1* (containing WT levels of MGDG) plants are defective for SAR. It is possible that a total threshold level of these galactolipids is important to generate AzA sufficient to induce SAR. This is supported by the fact that both MGDG and DGDG lipids are able to generate AzA and its precursor, 9-oxononanoic acid (ONA), when exposed to superoxide radical under in vitro conditions (Figure S5B). Notably, MGDG contained higher basal levels of ONA and AzA compared to DGDG, but DGDG accumulated higher proportion of AzA after treatment with superoxide radical (Figure S5B). These results, together with the cumulative observations that much of the cellular pool of AzA remains bound to lipids (Yu et al., 2013), only a small portion of 18:1 FA is converted to AzA (Yu et al., 2013 and this study), and the normal release of free FA in SAR and AzA compromised *mgd1*, *dgd1*, and *dgd1::GT* plants, suggest that pathogen-inducible AzA synthesis might occur via the oxidation of C18 FAs on MGDG and DGDG lipids rather than free FAs and that an AzA-DGDG derivative might facilitate the induction of *GLY1* and *GLI1* genes. Indeed, AzA functions upstream of G3P, and both *mgd1* and *dgd1* plants are compromised in pathogen-responsive G3P accumulation. However, at this point, we are unable to rule out a role for free FA in AzA biosynthesis, since both *mgd1* and *dgd1* are impaired in pathogen-induced ROS accumulation, which can generate AzA from FAs under in vitro conditions (Figure S5B; Yu et al., 2013).

Consistent with the notion that SAR requires the concomitant activation of both the SA and NO/ROS branches, exogenous application of SA did not restore the defective SAR in *dgd1* plants. In contrast, G3P application did confer SAR in *dgd1* plants, likely because G3P-conferred SAR only requires basal levels of SA and *dgd1* plants are not affected in basal SA levels. Notably, petiole exudates from both *mgd1* and *dgd1* plants were able to confer SAR on WT, though not on themselves, suggesting that these mutants are able to generate signal(s) upstream of galactolipid-mediated NO production (Figure S4). Identification of this signal(s) would help unravel the role that DGDG plays in pathogen-induced SA and NO accumulation.

EXPERIMENTAL PROCEDURES

Plant Growth Conditions and Genotypes Used

Plants were grown in MTPS 144 Conviron walk-in chambers at 22°C, 65% relative humidity, and 14 hr photoperiod. These chambers were equipped with cool white fluorescent bulbs (Sylvania, FO96/841/XP/ECO). The *mgd1-1*, *dgd1-1*, and transgenic plants expressing *DGD1* or the bacterial enzyme glycosyltransferase have been described before (Jarvis et al., 2000; Hölzl et al., 2006; Aronsson et al., 2008). The *mgd1 dgd1* double-mutant plants were obtained by pollinating flowers of the *mgd1* plant with pollen from *dgd1* plants. The double mutants were identified based on FA profile as well as genotype analysis.

Detailed experimental procedures are included in the Supplemental Experimental Procedures.

SUPPLEMENTAL INFORMATION

Supplemental Information includes Supplemental Experimental Procedures and five figures and can be found with this article online at http://dx.doi.org/10.1016/j.celrep.2014.10.069.

AUTHOR CONTRIBUTIONS

The bulk of the SAR experiments, expression analysis, G3P and AzA quantifications, and NO analysis were carried out by Q.-m.G. with help from Y.X. and C.W. Lipid and fatty acid analyses were carried out by K.Y. with help from Q.-m.G. AzA transport assay was carried out by K.Y. EPR experiments were carried out by M.B.S. with help from Q.-m.G. D.N. estimated SA. P.K. and A.K. supervised the project and wrote the manuscript with help from all the authors.

ACKNOWLEDGMENTS

We thank Georg Hölzl and Peter Dörmann for *dgd1* complemented lines and *dgd2* seeds, Henrik Aronsson for *mgd1* seeds, John Johnson for help with gas chromatography, Andrew Gifford and Joanna Fowler for ^{14}C-AzA, Joanne Holden for help with SA analysis, and Ludmila Lapchyk for technical help. We thank Christoph Benning for useful advice on galactolipid profiling and Peter Dörmann, David Wendehenne, Maelor Davies, Wolf-Dieter Reiter, and Meenakshi Upreti for useful suggestions. This work was supported by grants from National Science Foundation (IOS#0749731, MCB#0421914) and Kentucky Science and Engineering Foundation (2930-RDE-016).

Received: June 2, 2014
Revised: August 7, 2014
Accepted: October 30, 2014
Published: November 26, 2014

REFERENCES

Aronsson, H., Schöttler, M.A., Kelly, A.A., Sundqvist, C., Dörmann, P., Karim, S., and Jarvis, P. (2008). Monogalactosyldiacylglycerol deficiency in Arabidopsis affects pigment composition in the prolamellar body and impairs thylakoid membrane energization and photoprotection in leaves. Plant Physiol. *148*, 580–592.

Awai, K., Maréchal, E., Block, M.A., Brun, D., Masuda, T., Shimada, H., Takamiya, K., Ohta, H., and Joyard, J. (2001). Two types of MGDG synthase genes, found widely in both 16:3 and 18:3 plants, differentially mediate galactolipid syntheses in photosynthetic and nonphotosynthetic tissues in *Arabidopsis thaliana*. Proc. Natl. Acad. Sci. USA *98*, 10960–10965.

Chanda, B., Xia, Y., Mandal, M.K., Yu, K., Sekine, K.T., Gao, Q.M., Selote, D., Hu, Y., Stromberg, A., Navarre, D., et al. (2011). Glycerol-3-phosphate is a critical mobile inducer of systemic immunity in plants. Nat. Genet. *43*, 421–427.

Chaturvedi, R., Krothapalli, K., Makandar, R., Nandi, A., Sparks, A.A., Roth, M.R., Welti, R., and Shah, J. (2008). Plastid omega3-fatty acid desaturase-

dependent accumulation of a systemic acquired resistance inducing activity in petiole exudates of *Arabidopsis thaliana* is independent of jasmonic acid. Plant J. *54*, 106–117.

Chen, L.-J., and Li, H.-M. (1998). A mutant deficient in the plastid lipid DGD is defective in protein import into chloroplasts. Plant J. *16*, 33–39.

Christensen, L.P. (2009). Galactolipids as potential health promoting compounds in vegetable foods. Recent Pat Food Nutr Agric *1*, 50–58.

Dörmann, P., Balbo, I., and Benning, C. (1999). *Arabidopsis* galactolipid biosynthesis and lipid trafficking mediated by DGD1. Science *284*, 2181–2184.

Froehlich, J.E., Benning, C., and Dörmann, P. (2001). The digalactosyldiacylglycerol (DGDG) synthase DGD1 is inserted into the outer envelope membrane of chloroplasts in a manner independent of the general import pathway and does not depend on direct interaction with monogalactosyldiacylglycerol synthase for DGDG biosynthesis. J. Biol. Chem. *276*, 31806–31812.

Gao, Q.-M., Kachroo, A., and Kachroo, P. (2014). Chemical inducers of systemic immunity in plants. J. Exp. Bot. *65*, 1849–1855.

Hölzl, G., Witt, S., Kelly, A.A., Zähringer, U., Warnecke, D., Dörmann, P., and Heinz, E. (2006). Functional differences between galactolipids and glucolipids revealed in photosynthesis of higher plants. Proc. Natl. Acad. Sci. USA *103*, 7512–7517.

Jarvis, P., Dörmann, P., Peto, C.A., Lutes, J., Benning, C., and Chory, J. (2000). Galactolipid deficiency and abnormal chloroplast development in the *Arabidopsis MGD synthase 1* mutant. Proc. Natl. Acad. Sci. USA *97*, 8175–8179.

Jung, H.W., Tschaplinski, T.J., Wang, L., Glazebrook, J., and Greenberg, J.T. (2009). Priming in systemic plant immunity. Science *324*, 89–91.

Kachroo, A., and Robin, G.P. (2013). Systemic signaling during plant defense. Curr. Opin. Plant Biol. *16*, 527–533.

Kelly, A.A., and Dörmann, P. (2004). Green light for galactolipid trafficking. Curr. Opin. Plant Biol. *7*, 262–269.

Kelly, A.A., Froehlich, J.E., and Dörmann, P. (2003). Disruption of the two digalactosyldiacylglycerol synthase genes *DGD1* and *DGD2* in Arabidopsis reveals the existence of an additional enzyme of galactolipid synthesis. Plant Cell *15*, 2694–2706.

Klaus, D., Härtel, H., Fitzpatrick, L.M., Froehlich, J.E., Hubert, J., Benning, C., and Dörmann, P. (2002). Digalactosyldiacylglycerol synthesis in chloroplasts of the Arabidopsis dgd1 mutant. Plant Physiol. *128*, 885–895.

Kobayashi, K., Kondo, M., Fukuda, H., Nishimura, M., and Ohta, H. (2007). Galactolipid synthesis in chloroplast inner envelope is essential for proper thylakoid biogenesis, photosynthesis, and embryogenesis. Proc. Natl. Acad. Sci. USA *104*, 17216–17221.

Mandal, M.K., Chandra-Shekara, A.C., Jeong, R.-D., Yu, K., Zhu, S., Chanda, B., Navarre, D., Kachroo, A., and Kachroo, P. (2012). Oleic acid-dependent modulation of NITRIC OXIDE ASSOCIATED1 protein levels regulates nitric oxide-mediated defense signaling in *Arabidopsis*. Plant Cell *24*, 1654–1674.

Shah, J., and Zeier, J. (2013). Long-distance communication and signal amplification in systemic acquired resistance. Front Plant Sci *4*, 30.

Wang, R., Furumoto, T., Motoyama, K., Okazaki, K., Kondo, A., and Fukui, H. (2002). Possible antitumor promoters in Spinacia oleracea (spinach) and comparison of their contents among cultivars. Biosci. Biotechnol. Biochem. *66*, 248–254.

Wang, C., El-Shetehy, M., Shine, M.B., Yu, K., Navarre, D., Wendehenne, D., Kachroo, A., and Kachroo, P. (2014). Free radicals mediate systemic acquired resistance. Cell Rep *7*, 348–355.

Wendehenne, D., Gao, Q.-M., Kachroo, A., and Kachroo, P. (2014). Free radical-mediated systemic immunity in plants. Curr. Opin. Plant Biol. *20*, 127–134.

Xia, Y., Yu, K., Navarre, D., Seebold, K., Kachroo, A., and Kachroo, P. (2010). The *glabra1* mutation affects cuticle formation and plant responses to microbes. Plant Physiol. *154*, 833–846.

Xia, Y., Yu, K., Gao, Q.-M., Wilson, E.V., Navarre, D., Kachroo, P., and Kachroo, A. (2012). Acyl CoA binding proteins are required for cuticle formation and plant responses to microbes. Front Plant Sci *3*, 224–242.

Yu, K., Soares, J.M., Mandal, M.K., Wang, C., Chanda, B., Gifford, A.N., Fowler, J.S., Navarre, D., Kachroo, A., and Kachroo, P. (2013). A feedback regulatory loop between G3P and lipid transfer proteins DIR1 and AZI1 mediates azelaic-acid-induced systemic immunity. Cell Rep *3*, 1266–1278.

Zoeller, M., Stingl, N., Krischke, M., Fekete, A., Waller, F., Berger, S., and Mueller, M.J. (2012). Lipid profiling of the Arabidopsis hypersensitive response reveals specific lipid peroxidation and fragmentation processes: biogenesis of pimelic and azelaic acid. Plant Physiol. *160*, 365–378.